Optimal Antenna Spacings for Uncoded Space-Time Labelling Diversity Systems with Linear and Non-Linear Antenna Configurations

Sulaiman Saleem Patel*, Tahmid Quazi†, Hongjun Xu‡
School of Engineering, University of KwaZulu-Natal, South Africa
*sulaiman.s.patel@gmail.com
†quazit@ukzn.ac.za
‡xuh@ukzn.ac.za

***Abstract*—Uncoded Space-Time Labelling Diversity (USTLD) is a recent technique that has been applied to multiple-input, multiple-output (MIMO) systems to improve their error performance. However, the presence of multiple antennas leads to correlation, resulting in a performance degradation. Given that 5G systems aim to operate with large-scale antenna arrays and in the millimetre-wave frequency spectrum, antenna correlation is highly likely in next-generation MIMO systems. It is thus insightful to predict the optimal antenna spacing required to balance robustness to correlation with small form factor in USTLD systems. This paper investigates the cases of densely arranged, linearly arranged and equispaced antenna configurations to propose an optimal antenna spacing for each configuration. The results presented indicate that the optimal spacings are 0.3λ for dense antenna arrays, 0.4λ for linearly arranged antenna arrays and 0.3λ for equispaced antennas, where λ is the transmission carrier wavelength.**

***Index Terms*—antenna spacing, correlation analysis, labelling diversity, MIMO systems**

I. Introduction

High link reliability, low latencies and energy efficiency are among the key goals for the fifth generation (5G) of wireless communication systems [1]. A common approach to increase the reliability of wireless communication systems in the presence of multipath fading is to introduce diversity to the system at the physical layer [2]. Uncoded Space-Time Labelling Diversity (USTLD) [3] is a recently proposed scheme which achieves three levels of diversity: labelling diversity, time diversity and antenna diversity. Labelling diversity is achieved by transmitting the same binary data over two time slots using symbols from two different constellation mappings. The binary mappers are designed such that adjacent symbols in each constellation map are spaced further apart in subsequent maps. This allows detection to be based on symbol pairs instead of individual symbols. In doing so, error performance is improved in a similar manner to conventional error correction codes [4], despite USTLD being an uncoded system. Time diversity is achieved by transmitting these symbols over two time slots.

Antenna diversity is achieved by adopting a multiple-input, multiple-output (MIMO) structure, which creates more signal paths between transmitter and receiver, each of which experiences independent fading. Ideally, these signal paths are independent and identically distributed (i.i.d.). The use of multiple signal paths leads to lower error rates when compared to a single path [2], [4]. The original USTLD model in [3] was constrained to a system with two transmit antennas and any arbitrary N_{Rx} receive antennas. This was recently extended to allow for any N_{Tx} transmit antennas in [5]. As with all MIMO systems, conventional analysis of $N_{\text{Tx}} \times N_{\text{Rx}}$ USTLD systems assumes the ideal case of i.i.d. signal paths. However, this assumption is invalid if the spacing between antennas is less than half the wavelength of the transmission carrier (λ) [6]. Due to the inverse proportionality between wavelength and frequency [6], [7], antenna correlation becomes more likely at higher transmission frequencies, such as the millimetre wave frequency spectrum that has been proposed for 5G [8]. This has prompted studies into the affects of spatial correlation on USTLD systems [6], [9].

The simplest case of correlation analysis is to consider the dual-correlated channel [10], i.e. the case of two correlated receive antennas. USTLD systems have previously been studied under these conditions in [6], wherein the key finding was that they are more susceptible to antenna correlation than the comparable well-known Alamouti space-time block coded scheme [11]. This study was extended in [9], which considered correlation between any number of transmit and receive antennas. The work in [9] uses the technique proposed by [12] to derive a statistical model for the analysis of USTLD systems. Using this technique, it is shown that the identical, correlated channels may be modelled as eigenvalue-weighted, non-identical, uncorrelated channels for statistical analysis [9], [12]. In addition, [9] shows that USTLD systems are more sensitive to transmit antenna correlation than receive antenna correlation; and proposes an optimal spacing of 0.4λ for linearly arranged antenna arrays (LAAAs). This optimal spacing theoretically balances robustness to performance degradation as a result of antenna correlation and small form factor, providing a useful guideline to implementing practical USTLD systems.

The study of [9] focusses on LAAAs, modelling the pairwise antenna correlation in terms of the physical space between antennas. However, it is often impractical to arrange antennas linearly when there is limited space available. This is especially relevant when considering large antenna arrays,

such as the Massive MIMO system architecture [13] which has been proposed for 5G. Since the study of [9] was constrained to only linear antenna configurations, this paper expands the study to also consider non-linear configurations, and determine optimal antenna spacings under these configurations. In particular, the antenna configurations described by the constant correlation [14] and exponential correlation [13], [14] models are considered. These models are appropriate for modelling dense antenna arrays and equispaced antenna configurations respectively.

The remainder of this paper is structured as follows: Section II presents the system model for correlated $N_{\text{Tx}} \times N_{\text{Rx}}$ USTLD systems, and Section III presents the analytical union bound of the average bit error probability (ABEP) to theoretically model the system. Section IV presents numerical results to verify the theoretical expression in Section III, as well as determine the optimal antenna spacings for USTLD systems with non-linear antenna configurations. Finally, Section V concludes this paper.

In terms of notation, this paper denotes scalars in italics, vectors in bold lowercase and matrices in bold uppercase. The operators $\oplus$, $|\cdot|$, $\|\cdot\|$, $\mathcal{E}\{\cdot\}$, $(\cdot)^{\text{H}}$ and $(\cdot)^{\text{T}}$ respectively denote the binary exclusive-or, absolute value, vector Frobenius norm, statistical expectation, Hermitian and transpose. The function $\aleph(\mathbf{A})$ returns the vector of all eigenvalues of matrix $\mathbf{A}$ through the process of eigenvalue decomposition.

II. System Model

A. Transmission and Detection Models

This paper considers the $N_{\text{Tx}} \times N_{\text{Rx}}$ USTLD system model given by [9], which is constrained such that $N_{\text{Tx}} \leq N_{\text{Rx}}$. A stream of mN_{Tx} information bits is transmitted across two time slots. Every m consecutive bits are used to define a codeword, c_i, $i \in [1 : N_{\text{Tx}}]$. Thus, the information bitstream may be denoted as $\mathbf{c} = \begin{bmatrix} c_1 & c_2 & \cdots & c_{N_{\text{Tx}}} \end{bmatrix}^{\text{T}}$. During time slot k, $k \in [1 : 2]$, each codeword c_i is mapped using binary mapper Ω_k to produce symbol $\Omega_k(c_i)$. The $N_{\text{Tx}} \times 1$ vector of all symbols to be transmitted in time slot t is denoted $\Omega_k(\mathbf{c})$. The generation of $\Omega_1(\mathbf{c})$ and $\Omega_2(\mathbf{c})$ is illustrated in Fig. 1. This paper focusses on square quadrature amplitude modulation (QAM) and phase shift keyed (PSK) constellations, due to the existence of binary mappers that achieve labelling diversity for these modulation schemes [3], [15]. For 16QAM, the mapping scheme proposed by [15] (illustrated in Fig. 2) is used. This is found to be optimal by both [3] and [15]. For PSK constellations, the suboptimal heuristic design technique of [3] is used. The symbol constellations are power-normalised to ensure that $\mathcal{E}\left\{|\Omega_k(c_i)|^2\right\} = 1$, $k \in [1 : 2]$, $i \in [1 : N_{\text{Tx}}]$.

Hence, the $N_{\text{Rx}} \times 1$ received signal vector, $\mathbf{r}$, in time slot k is then given by

$$\mathbf{r}_k = \sqrt{\frac{\gamma}{N_{\text{Tx}}}}\, \mathbf{H}_k\, \Omega_k(\mathbf{c}) + \mathbf{n}_k, \quad k \in [1 : 2], \tag{1}$$

where γ is the total average signal-to-noise ratio (SNR) of the transmission. Additive white Gaussian noise present at the receiver is denoted by $N_{\text{Rx}} \times 1$ vector $\mathbf{n}$ and follows a complex normal distribution with zero mean and unit variance. $\mathbf{H}$ is the $N_{\text{Rx}} \times N_{\text{Tx}}$ matrix of complex coefficients to model the effect of multipath fading. This is assumed to follow a Nakagami-q amplitude distribution with zero mean and unit variance, the probability density function for which is $f_x(x) = \frac{x\left(1+q^2\right)}{q} \exp\left(-\frac{x^2\left(1+q^2\right)^2}{4q^2}\right) I_0\left(\frac{x^2\left(1-q^4\right)}{4q^2}\right)$, where x is the fading amplitude, $I_0(\cdot)$ is the modified zeroth-order Bessel function of the first kind [2] and the fading parameter, q, is the energy ratio of the quadrature component of the fading to its in-phase component [9]. The Nakagami-q fading model is used ahead of the more common Rayleigh fading model as it allows more insight into the worst-case error performance of the system [9]. The fading channels are assumed to be correlated, frequency-flat and may be either fast fading or quasi-static over the duration of the two time slots. A uniform phase distribution is assumed for both noise and fading.

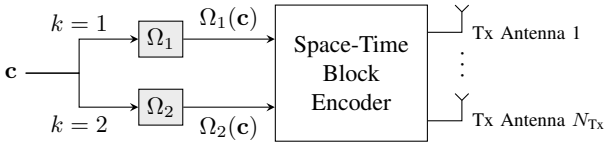

Fig. 1. Block Diagram of a USTLD Transmitter

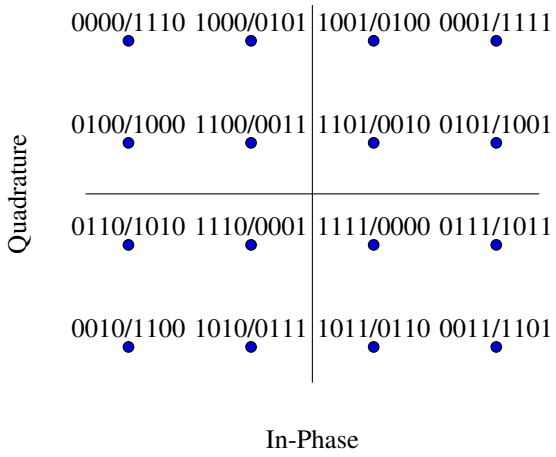

Fig. 2. 16QAM Binary Constellation Mapping. Key: Ω_1/Ω_2

At the receiver, it is assumed that a pilot signal and training sequence is utilised to attain perfect channel state information. The estimated codeword vector, $\tilde{\mathbf{c}} = \begin{bmatrix} \tilde{c}_1 & \tilde{c}_2 & \cdots & \tilde{c}_{N_{\text{Tx}}} \end{bmatrix}^{\text{T}}$, is then given by

$$\tilde{\mathbf{c}} = \underset{\substack{\hat{c}_i \in [0:2^m-1] \\ i \in [1:N_{\text{Tx}}]}}{\arg\min} \sum_{k=1}^{2} \left\| \mathbf{r}_k = \sqrt{\frac{\gamma}{N_{\text{Tx}}}}\, \mathbf{H}_k\, \Omega_k(\hat{\mathbf{c}}) \right\|^2, \tag{2}$$

where $\hat{\mathbf{c}} = \begin{bmatrix} \hat{c}_1 & \hat{c}_2 & \cdots & \hat{c}_{N_{\text{Tx}}} \end{bmatrix}^{\text{T}}$ is a vector comprising of candidate codewords that may have been transmitted.

B. Correlation Model

Literature shows that two of the most popular models for analysing channel correlation are the separable model [12] and the canonical model [16], [17]. The latter generally provides a better fit to measured data and is often used to model channel capacity. However, [16] shows that for antenna correlation, both models are equivalent and reduce to the separable (Kronecker) model. Using the Kronecker model, the correlated channel matrix in time slot k, $k \in [1:2]$, is

$$\mathbf{H}_k = \mathbf{R}_{\text{Rx}}^{\frac{1}{2}} \, \mathbf{V}_k \left(\mathbf{R}_{\text{Tx}}^{\frac{1}{2}}\right)^{\text{T}}, \tag{3}$$

where $\mathbf{V}_k$ is a virtual, uncorrelated channel matrix in time slot k and $\mathbf{R}_{\text{Tx}}$ and $\mathbf{R}_{\text{Rx}}$ are, respectively, the $N_{\text{Tx}} \times N_{\text{Tx}}$ transmit antenna correlation matrix and the $N_{\text{Rx}} \times N_{\text{Rx}}$ receive antenna correlation matrix. $\mathbf{R}_{\text{Tx}}$ may be explicitly written as

$$\mathbf{R}_{\text{Tx}} = \begin{bmatrix} 1 & \rho_{\text{Tx}}^{(1,2)} & \cdots & \rho_{\text{Tx}}^{(1,N_{\text{Tx}})} \\ \rho_{\text{Tx}}^{(2,1)} & 1 & \cdots & \rho_{\text{Tx}}^{(2,N_{\text{Tx}})} \\ \vdots & \vdots & \ddots & \vdots \\ \rho_{\text{Tx}}^{(N_{\text{Tx}},1)} & \cdots & \rho_{\text{Tx}}^{(N_{\text{Tx}},N_{\text{Tx}}-1)} & 1 \end{bmatrix}, \tag{4}$$

where $\rho_{\text{Tx}}^{(a,b)}$ is the magnitude of the correlation coefficient between the a-th and b-th transmit antennas. $\mathbf{R}_{\text{Rx}}$ is similarly defined in terms of the correlation coefficients between the c-th and d-th receive antennas, $\rho_{\text{Rx}}^{(c,d)}$. As shown in (4), the correlation matrices are diagonally symmetrical such that $\rho_{\text{Tx}}^{(i,j)} = \rho_{\text{Tx}}^{(j,i)}, i \neq j, i, j \in [1 : N_{\text{Tx}}]$, and similarly, $\rho_{\text{Rx}}^{(i,j)} = \rho_{\text{Rx}}^{(j,i)}, i \neq j, i, j \in [1 : N_{\text{Rx}}]$.

It is shown in [18] that the correlation between two antennas may be given by

$$\rho = J_0\left(2\pi \frac{\mu}{\lambda}\right), \tag{5}$$

where $J_0(\cdot)$ is the (unmodified) zeroth-order Bessel function of the first kind, μ is the distance between the two antennas and λ is the wavelength of the transmission carrier. This may be used to determine the elements of $\mathbf{R}_{\text{Tx}}$ and $\mathbf{R}_{\text{Rx}}$ depending on the physical configuration of the antennas at the transmitter and receiver respectively. In this paper, three antenna configuration models are considered (as illustrated in Fig. 3):

1) Dense Antenna Arrays: As per [17], for dense arrays where all antennas are close together, the correlation between each pair of antennas is approximately constant. In this case, the spacings between all antennas are also approximately constant. Hence, the correlation coefficients are given by

$$\rho^{(i,j)} = \begin{cases} \rho; & i \neq j \\ 1; & i = j \end{cases} \tag{6}$$

2) Linearly Arranged Antenna Arrays: When antennas are arranged linearly, (5) is used directly when calculating the correlation coefficient [9]. Hence, $\rho^{(i,j)} = J_0\left(\frac{2\pi}{\lambda}\mu^{(i,j)}\right)$, where $\mu^{(i,j)}$ is the distance between antennas i and j. As in [9], this paper considers linear configurations where the spacing between adjacent antennas is constant (i.e. $\mu_{\text{Rx}}^{(a,a+1)} = \mu_{\text{Rx}}$, $a \in [1 : N_{\text{Rx}} - 1]$, and similarly, $\mu_{\text{Tx}}^{(b,b+1)} = \mu_{\text{Tx}}$, $b \in [1 : N_{\text{Tx}} - 1]$). Thus, for the illustration in Fig. 3(b), $\mu^{(1,2)} = \mu^{(2,3)} = \mu$ and $\mu^{(1,3)} = 2\mu$.

3) Equispaced Antennas: When antennas are arranged such that they are approximately equispaced, the correlation between them decreases exponentially [17]. An example of such an arrangement for three antennas is shown in Fig. 3(c), where $\mu^{(1,2)} = \mu^{(2,3)} = \mu^{(1,3)} = \mu$. Under these conditions, the correlation coefficient is given by

$$\rho^{(i,j)} = \rho^{|i-j|} \tag{7}$$

and ρ is calculated using (5).

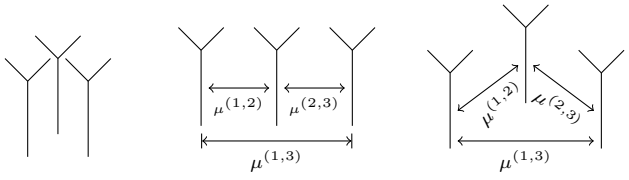

(a) Dense Arrays (b) Linear Arrays (c) Equispaced Arrays

Fig. 3. Illustrations of Antenna Configurations Studied

III. Analysis of Average Bit Error Performance

The ABEP of an $N_{\text{Tx}} \times N_{\text{Rx}}$ USTLD system in correlated Nakagami-q channels has been fully derived in literature, and the reader is referred to [9] for a more detailed discussion than what is presented in this paper.

As per [5], [9], the union bound on the ABEP for $N_{\text{Tx}} \times N_{\text{Rx}}$ USTLD systems is given by

$$P_b(\gamma) \leq \frac{1}{mN_{\text{Tx}}2^m} \sum_{c \in \boldsymbol{\xi}} \sum_{\substack{\tilde{\mathbf{c}} \in \boldsymbol{\xi} \\ \mathbf{c} \neq \tilde{\mathbf{c}}}} \delta(\mathbf{c}, \tilde{\mathbf{c}}) P\left(\mathbf{c} \to \tilde{\mathbf{c}}\right), \tag{8}$$

where $\boldsymbol{\xi}$ is the set of all $2^{mN_{\text{Tx}}}$ possible transmitted codeword vectors. $\delta(\mathbf{c}, \tilde{\mathbf{c}})$ is the total number of bit error between transmitted codeword vector $\mathbf{c}$ and estimated codeword vector $\tilde{\mathbf{c}}$. $P\left(\mathbf{c} \to \tilde{\mathbf{c}}\right)$ is the pairwise error probability (PEP) of incorrectly detecting $\mathbf{c}$ as $\tilde{\mathbf{c}}$.

The number of bit errors may be expressed as

$$\delta(\mathbf{c}, \tilde{\mathbf{c}}) = \sum_{i=1}^{N_{\text{Tx}}} \sum_{j=1}^{m} b_{c_i}^{(j)} \oplus b_{\tilde{c}_i}^{(j)}, \tag{9}$$

where $b_{c_i}^{(j)}$ denotes the j-th bit of i-th array element in $\mathbf{c}$, and similarly for $b_{\tilde{c}_i}^{(j)}$.

As shown in (3), the Kronecker correlation model shows that the correlated channel matrix during the k-th time slot, $\mathbf{H}_k$, $k \in [1:2]$, may be expressed in terms of an artificial, uncorrelated channel matrix $\mathbf{V}_k$. By adopting this model and applying the analysis techniques of [12], the authors of [9] show that the PEP for USTLD systems in *correlated* channels

is found by using the result found for *uncorrelated* channels. This is given by [9, Eq. (23)]

$$P\left(\mathbf{c}\to\tilde{\mathbf{c}}\right)\approx\frac{1}{4n}\prod_{k=1}^{2}\prod_{j=1}^{N_{\text{Rx}}}\mathcal{M}_k\left(\frac{1}{2},\alpha_j\beta_k\right)+\frac{1}{2n}\sum_{m=1}^{n-1}\prod_{k=1}^{2}\prod_{j=1}^{N_{\text{Rx}}}\mathcal{M}_k\left(\frac{1}{2}\csc^2\left(\frac{m\pi}{2n}\right),\alpha_j\beta_k\right), \tag{10}$$

where n is an arbitrarily large integer $n > 10$. $\mathcal{M}_k(s,x)$ is the moment generating function (MGF) of the Nakagami-q distribution [2], given in (11). The second argument in the MGF expressions shows that the PEP is determined by the N_{Rx} eigenvalues of the receive antenna correlation matrix, α_j, $j \in [1 : N_{\text{Rx}}]$, and the non-zero eigenvalue of the squared-distance weighted transmit antenna correlation matrix in each time slot, β_k, $k \in [1 : 2]$. The operations to produce these eigenvalues are explicitly given in (12) and (13).

$$\mathcal{M}_k(s,x)=\left[1+\frac{s\gamma x}{N_{\text{Tx}}}+\left(\frac{sq\gamma x}{N_{\text{Tx}}(1+q^2)}\right)^2\right]^{-\frac{1}{2}} \tag{11}$$

$$\begin{bmatrix}\alpha_1 & \cdots & \alpha_{N_{\text{Rx}}}\end{bmatrix}^{\text{T}}=\aleph\{\mathbf{R}_{\text{Rx}}\} \tag{12}$$

$$\beta_k=\aleph\{\mathbf{d}_k\cdot\mathbf{d}_k^{\text{H}}\cdot\mathbf{R}_{\text{Tx}}\},\ \beta_k\neq 0, k\in[1:2] \tag{13}$$

In (13), $\mathbf{d}_k$ is the vector of distances between the symbols represented by $\mathbf{c}$ and $\tilde{\mathbf{c}}$ using mapper Ω_k, $k \in [1 : 2]$, which is given by

$$\mathbf{d}_k=\Omega_k(\mathbf{c})-\Omega_k(\tilde{\mathbf{c}})=\begin{bmatrix}\Omega_k(c_1)-\Omega_k(\tilde{c}_1)\\ \vdots \\ \Omega_k(c_{N_{\text{Tx}}})-\Omega_k(\tilde{c}_{N_{\text{Tx}}})\end{bmatrix} \tag{14}$$

The authors emphasise that in (13), $\mathbf{d}_k \cdot \mathbf{d}_k^{\text{H}} \cdot \mathbf{R}_{\text{Tx}}$ has rank one and thus there is only one non-zero eigenvalue for each value of $k, k \in [1 : 2]$, as shown by [12].

The final ABEP for $N_{\text{Tx}} \times N_{\text{Rx}}$ USTLD systems in Nakagami-q fading is thus obtained by substituting (9) and (10) in (8).

IV. Results

The results presented in this section use Monte Carlo simulations to predict the behaviour of the USTLD systems considered. The first set of results, shown in Fig. 4, verifies that the analytical union bound on the ABEP presented in Section III converges to the simulated results. Results are shown for dense antenna arrays, linearly arranged antenna arrays (LAAAs) and equispaced antenna arrays, as well as for 8PSK, 16PSK and 16QAM. The Nakagami-q fading coefficient (q), transmit antenna spacing (μ_t), receive antenna spacing (μ_r) and antenna configuration for each of the systems presented are summarised in Table I.

The next set of results studies the effects of transmit and receive antenna correlation independently on USTLD systems, for each of the three antenna configurations considered in this paper. This approach may be used to obtain a theoretically optimal antenna spacing for the system, as was done in [9].

TABLE I
Simulation Parameters for USTLD Systems presented in Fig. 4

Modulation	q	μ_t	μ_r	Antenna Config.
16PSK	0.5	0.7λ	0.4λ	2×4 (Dense)
8PSK	0.1	0.25λ	0.75λ	3×5 (Equispaced)
8PSK	0.9	0.25λ	0.75λ	3×5 (Linear)
16QAM	0.8	0.24λ	0.3λ	2×3 (Linear)

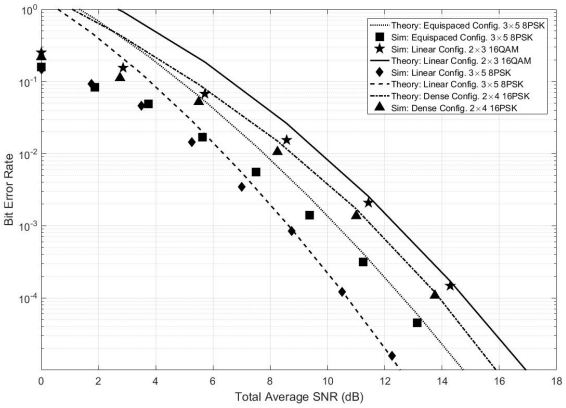

Fig. 4. Verification of Theoretical Results using Monte Carlo Simulations

Intuitively, it is expected that when antennas are spaced close together, the correlation between them is high. This may be confirmed using practical values of (5). Thus, it is expected that MIMO systems with closely spaced antennas perform worse than those with antennas spaced further apart. In Figs. 5–7, results are presented to show the affect of changing antenna spacing on the error performance of USTLD systems. The gradient of the curves indicates the *rate at which error performance improves as antennas are spaced further apart.* The results are presented for dense antenna arrays (Fig. 5), LAAAs (Fig. 6) and equispaced antennas (Fig. 7). Antenna spacings are presented in terms of the transmission carrier wavelength (λ) to generalise results across all frequencies. The results are presented for 8PSK, 16PSK and 16QAM and different MIMO structures.

In analysing the results in Figs. 5–7, it is found that performance improves rapidly when antennas are close together. This is evident by the steep gradients of curves in the region $0 < \mu \leq 0.3\lambda$ in Figs. 5 and 7, as well as the region $0 < \mu \leq 0.4\lambda$ in Fig. 6. Curves are then found to exhibit a much flatter gradient, indicating that further increases to antenna spacing do not result in much error performance improvement. Thus, it may be concluded that the upper bound of the 'steep region' for each antenna configuration represents a theoretical optimal antenna spacing, $\mu^{(\text{opt})}$, which balances robustness to spatial correlation and small form factor. For linear configurations, Fig. 6 shows that $\mu^{(\text{opt., linear})} = 0.4\lambda$, which is in agreement with the results attained in [9]. For dense and equispaced antenna arrays, Figs. 5 and 7 indicate that $\mu^{(\text{opt., dense})} = \mu^{(\text{opt., equispaced})} = 0.3\lambda$ in both cases. Thus, these configurations are better suited than LAAAs for USTLD systems, as a lower value of $\mu^{(\text{opt.})}$ allows for smaller form factors to be achieved. However, it is further observed

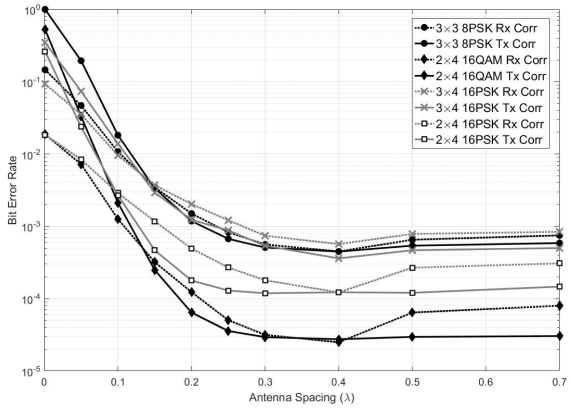

Fig. 5. Improvement of Error Performance in Dense Antenna Arrays ($q = 0.2, \gamma = 15$dB)

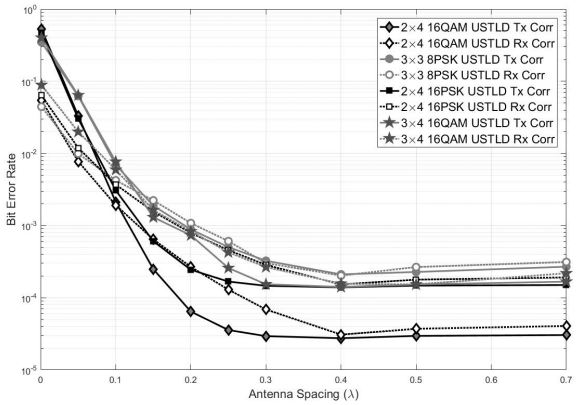

Fig. 6. Improvement of Error Performance in Linearly Arranged Antenna Arrays ($q = 0.2, \gamma = 15$dB)

that for dense arrays, there is a significant degradation in error performance that occurs when $\mu > 0.4\lambda$ (approximately half an order of magnitude). Upon careful inspection of the results, degradation in this region is observed for LAAAs and equispaced antennas as well, however the extent of the degradation is negligible. It may thus be concluded that the most optimal configuration for USTLD systems is to have equispaced antennas which are spaced 0.3λ apart from each other. It is also noted that for dense, linearly arranged and equispaced, the USTLD systems are more susceptible to transmit antenna correlation than receive antenna correlation. This is in agreement with the results in [9], which explains it mathematically. The reason USTLD systems are more sensitive to transmit antenna correlation is that the transmit antenna correlation matrix $\mathbf{R}_{\text{Tx}}$ is weighted by the distance product $\mathbf{d} \cdot \mathbf{d}^{\text{H}}$ before undergoing eigenvalue decomposition, as shown in (13). By contrast, (12) shows that the receive antenna correlation matrix $\mathbf{R}_{\text{Rx}}$ undergoes eigenvalue decomposition directly. Therefore, the eigenvalue product that is used in determining the PEP of correlated USTLD systems, given in (10), is affected more by the transmit antenna correlation matrix.

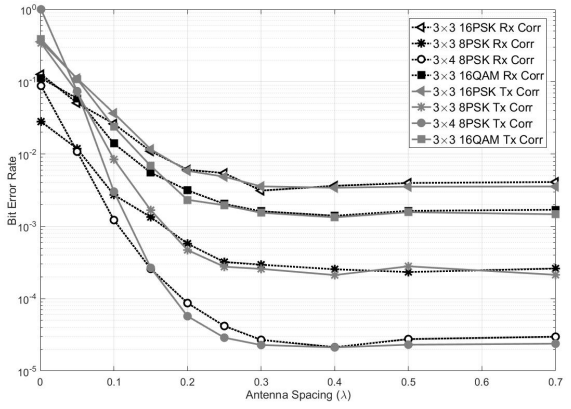

Fig. 7. Improvement of Error Performance in Equispaced Antenna Arrays ($q = 0.2, \gamma = 15$dB)

V. Conclusion

This paper presents a study of $N_{\text{Tx}} \times N_{\text{Rx}}$ USTLD systems in the presence of spatially correlated Nakagami-q channels. The correlation between antennas is shown to be a function of the distance between them and the physical arrangement of the antennas. Three configurations are presented: dense antenna arrays, linearly arranged antenna arrays and equispaced antennas. For each of the above configurations, the analytical expression for the union bound of the ABEP of correlated USTLD systems is validated using Monte Carlo simulations. These simulations show a tight fit in the high SNR region for different modulation schemes and MIMO structures (3×5 8PSK, 2×4 16PSK and 2×3 16QAM). A study is then conducted to determine the optimal antenna spacing, $\mu^{(\text{opt.})}$, for each physical configuration. Linear antenna arrays are shown to be the worst antenna configuration, as $\mu^{(\text{opt., linear})} = 0.4\lambda > \mu^{(\text{opt., dense})}, \mu^{(\text{opt., equispaced})}$. It is further shown that equispaced antenna configuration is the most optimal, and has optimal antenna spacing $\mu^{(\text{opt., equispaced})} = 0.3\lambda$. Future works in this area may consider testing the validity of the results in this paper by practically implementing $N_{\text{Tx}} \times N_{\text{Rx}}$ USTLD systems.

Acknowledgement

The primary author would like to firstly acknowledge God Almighty, without whom no achievements are possible. Thereafter, acknowledgement goes to Ahmad Khalid and Muhammed Zia Dawood for their assistance in proofreading and editing the manuscript, to his parents and family, and to the Telkom Centre of Excellence at UKZN for financially supporting this research.

References

[1] S. Zhang, X. Xu, Y. Wu, and L. Lu, "5G: Towards Energy-Efficient, Low-Latency and High-Reliable Communications Networks," in *2014 IEEE International Conference on Communication Systems*, Nov. 2014, pp. 197–201. DOI: 10.1109/ICCS.2014.7024793.

[2] M. K. Simon and M.-S. Alouini, *Digital Communication over Fading Channels, A Unified Approach to Performance Analysis*, 2nd ed. John Wiley & Sons, Inc., 2000.

[3] H. Xu, K. Govindasamy, and N. Pillay, "Uncoded Space-Time Labelling Diversity," *IEEE Communications Letters*, vol. 20, no. 8, pp. 1511–1514, Aug. 2016.

[4] S. Haykin and M. Moher, *Communication Systems*, 5th ed. John Wiley & Sons, Inc., 2010.

[5] S. S. Patel, T. Quazi, and H. Xu, "Full MIMO Uncoded Space Time Labelling Diversity with Low-Complexity Detection," provisionally accepted, *IET Communications*, 2017.

[6] ——, "Performance of Uncoded Space-Time Labelling Diversity in Dual-Correlated Rayleigh-Fading Channels," in *Proceedings of the Southern Africa Telecommunications Networks and Applications Conference (SATNAC)*, S. van Loggerenberg and J. Laureles, Eds., Freedom of the Seas Cruise Liner, Barcelona, Spain, Sep. 2017, pp. 68–72.

[7] A. Goldsmith, *Wireless Communications*. Cambridge University Press, 2005.

[8] T. S. Rappaport, S. Sun, R. Mayzus, H. Zhao, Y. Azar, K. Wang, G. N. Wong, J. K. Schulz, M. Samimi, and F. Gutierrez, "Millimeter wave mobile communications for 5g cellular: It will work!" *IEEE Access*, vol. 1, pp. 335–349, 2013. DOI: 10.1109/ACCESS.2013.2260813.

[9] S. S. Patel, T. Quazi, and H. Xu, "Error performance of Uncoded Space Time Labeling Diversity in spatially correlated Nakagami-q channels," *International Journal of Communication Systems*, vol. 31, no. 12, e3720, 2018. DOI: 10.1002/dac.3720.

[10] L. Fang, G. Bi, and A. C. Cot, "New method of performance analysis for diversity reception with correlated Rayleigh-fading signals," *IEEE Transactions on Vehicular Technology*, vol. 49, no. 5, pp. 1807–1812, 2000.

[11] S. Alamouti, "A Simple Transmit Diversity Technique for Wireless Communications," *IEEE Journal on Selected Areas in Communications*, vol. 16, no. 8, pp. 1451–1458, Oct. 1998.

[12] A. Hedayet, H. Shah, and A. Nosratinia, "Analysis of Space-Time Coding in Correlated Fading Channels," *IEEE Transactions on Wireless Communications*, vol. 4, no. 6, pp. 2882–2891, 2005.

[13] S. Albdran, A. Alshammari, and M. A. Matin, "Spectral and energy efficiency for massive MIMO systems using exponential correlation model," in *2017 IEEE 7th Annual Computing and Communication Workshop and Conference (CCWC)*, Jan. 2017, pp. 1–5. DOI: 10.1109/CCWC.2017.7868390.

[14] V. A. Aalo, "Performance of maximal-ratio diversity systems in a correlated Nakagami-fading environment," *IEEE Transactions on Communications*, vol. 43, no. 8, pp. 2360–2369, Aug. 1995, ISSN: 0090-6778. DOI: 10.1109/26.403769.

[15] H. Samra, Z. Ding, and P. Hahn, "Symbol Mapping Diversity Design for Multiple Packet Transmissions," *IEEE Transactions on Communications*, vol. 53, no. 5, pp. 810–817, May 2005.

[16] A. Moustakas, H. Baranger, L. Balents, A. Sengupta, and S. Simon, "Communication through a diffusive medium: Coherence and capacity," *Science*, vol. 287, pp. 287–290, 2000. DOI: 10.1126/science.287.5451.287.

[17] A. M. Tulino, A. Lozano, and S. Verdu, "Impact of antenna correlation on the capacity of multiantenna channels," *IEEE Transactions on Information Theory*, vol. 51, no. 7, pp. 2491–2509, Jul. 2005, ISSN: 0018-9448. DOI: 10.1109/TIT.2005.850094.

[18] N. Ebrahimi-Tofighi, M. Ardebilipour, and M. Shahabadi, "Receive and Transmit Array Antenna Spacing and Their Effect on the Performance of SIMO and MIMO Systems by using an RCS Channel Model," *International Journal of Electrical, Computer, Energetic, Electronic and Communication Engineering*, vol. 1, no. 12, pp. 1732–1736, 2007.

Sulaiman Saleem Patel attained his BScEng in Electronic Engineering *Summa Cum Laude* from UKZN in 2015. He is currently pursuing his PhD, after satisfying the requirements for a MScEng *Cum Laude* in 2015. Sulaiman is the President of the IEEE-Eta Kappa Nu Student Chapter (Mu Eta) at UKZN, a member of both the UKZN Telkom CoE and the UKZN Engineers Without Borders Chapter, as well as the postgraduate representative of the electrical, electronic and computer engineering department.